

Correlation between Photophysical Parameters and Gold–Gold Distances in Gold(I) (4-Pyridyl)ethynyl Complexes

Laura Rodríguez,[†] Montserrat Ferrer,[†] Ramon Crehuet,[‡] Josep Anglada,[‡] and João Carlos Lima^{*,§}

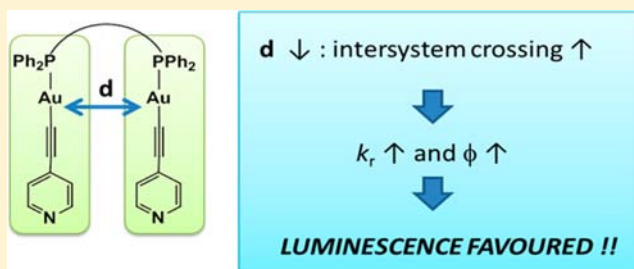
[†]Departament de Química Inorgànica, Universitat de Barcelona, Martí i Franquès 1-11, 08028 Barcelona, Spain

[‡]Institut de Química Avançada de Catalunya, IQAC–CSIC c/Jordi Girona 18-26, Barcelona 08034, Spain

[§]REQUIMTE, Departamento de Química, Centro de Química Fina e Biotecnologia, Universidade Nova de Lisboa, Quinta da Torre, 2829-516 Monte de Caparica, Portugal.

S Supporting Information

ABSTRACT: The systematic analysis of the luminescence of a series of alkynyl gold derivatives with general formulas $[(\text{diphos})(\text{AuC}\equiv\text{Cpy})_2]$ (diphosphane = 2,2'-bis-(diphenylphosphanyl)propane or dppip (1), bis-(diphenylphosphanyl)acetylene or dppa (2), 1,2-bis-(diphenylphosphanyl)ethane or dppe (3) and 1,4-bis-(diphenylphosphanyl)butane or dppb, (4), has shown a straightforward correlation between the Au(I)⋯Au(I) distance and the emission quantum yields and decaytimes. The analysis of the decaytimes, quantum yields and thus, the corresponding calculated rate constants demonstrated the existence of a correlation between Au(I)⋯Au(I) distance and the radiative rate constant for the deactivation of the emissive triplet states. It was concluded that the increased emission of these compounds results from the increase in spin–orbit coupling that favors the spin forbidden transition to the singlet ground state.



INTRODUCTION

During the past decade polynuclear gold(I) complexes, and in particular their photophysics, has attracted a considerable attention because of their potential applications to the field of photonic devices and nanomaterials.¹

The strong relativistic effects displayed by gold atoms, that is, the phenomenon associated to high-speed electrons moving close to the heavy atomic nucleus, confer them distinct properties.² An increase in the effective nuclear charge causes a contraction of the less-diffuse orbitals, whereas the more-diffuse orbitals expand due to the enhanced shielding effect by the contracted orbitals. Gold exhibits the maximum relativistic effect among their neighbors in the periodic table, which means that the extent of contraction in the 6s and 6p orbitals, and at the same time the expansion of 5d orbitals is the most significant.³ These effects are in the basis of the observation of aurophilic interactions between gold centers, which have attracted a growing attention and accelerated the development of gold(I) chemistry. This phenomenon (aurophilicity⁴) even became a model for the description of relativistic effects in closed-shell metals, of which gold(I) is the best example.^{5–7} Because of a similarity in energy and directionality between aurophilic interactions and hydrogen bonds, aurophilicity plays a key role in molecular aggregation in both solid state and solution.

The luminescence studies of gold(I) complexes are of particular interest due to the possibility offered of a straightforward way to study Au⋯Au interactions, which in some cases are reported to be the origin of the luminescence

behavior. Several examples found in the literature of structural and spectroscopic evidence of the effect of the aurophilic interactions on the observed luminescence induced scientists to carry out theoretical studies which intend to give the scientific community an explanation of the luminescence of gold compounds and its relation to aurophilicity through the Au⋯Au distance dependence of the luminescence features.^{8–10}

Yet, its nature has not been rationalized in a consensual and general view and continuous efforts in the assignment of the states responsible for the observed emissions are still needed.¹¹ The difficulties result in part of the extensive state mixing that occurs in metal complexes, which turns difficult to find simple assignments to the states, such as the presence of a low energy molecular orbital centered at Au⋯Au, which would be one of the orbitals involved in the lowest energy electronic transition observed in emission. This would constitute the ideal and straightforward assignment of an “aurophilic” emissive state. In addition, gold complexes without aurophilic interactions, as measured by X-ray crystallographic distances, sometimes show identical luminescence to the ones claimed to be unequivocal proof of aurophilic interactions. In fact, the luminescence is affected by the nature of the ligands, by the geometry around the metal center or by the presence of metal–metal interactions in the complexes, which in principle permits the rational design of complexes for specific applications. Nevertheless, the

Received: March 22, 2012

Published: June 28, 2012

conjunction in a gold complex of more than one of these conditions makes the assignments complicated.¹²

Gold alkynyl complexes usually exhibit intense low-energy absorptions in the UV–vis region originated mainly from alkynyl-centered $\pi-\pi^*$ ($C\equiv CR$) transition as well as charge transfer transitions between alkynyl ligands and metal ions or ancillary ligands.^{13–19} In a previous work,¹⁷ we have conducted a systematic analysis of the luminescence of a series of alkynyl gold derivatives, synthesized by us and we have found no straightforward relation between the existence of $Au(I)\cdots Au(I)$ interactions and the occurrence of emission. Thus, in order to go one step further, we have decided to analyze in detail the photophysical properties of some of the previously reported alkynyl phosphine gold compounds. On the other hand, theoretical calculations have been also carried out to assign the states responsible for this intriguing emission broad band to rationalize the observed experimental data.

Interestingly, experimental and theoretical data are in good agreement and provide an explanation of why aurophilic interactions favor the emission on these compounds.

EXPERIMENTAL SECTION

Physical Data. The overall emission quantum yields were recorded with an integrating sphere accessory for a Horiba–Jobin–Yvon SPEX Fluorolog 3.22 spectrofluorimeter. The samples were excited at 350 nm and the emission integrated in the range 400–650 nm. The decay times of the powders and X-ray $Au\cdots Au$ distances are retrieved from previous reported data.¹⁷ Decay times were measured with a laser flash photolysis LK60 Applied Photophysics system in emission mode, collecting the decay at 550 nm after laser pulse excitation at 355 nm at the Departamento de Química-Universidade Nova de Lisboa.

Computational Details. All calculations have been carried out using the Gaussian09 suite of programs.²⁰ Due to the large size of the molecules considered, the study of the electronic excited states has been done employing linear response time-dependent density functional theory (TD-DFT) with the CAM-B3LYP functional.²¹ This functional has been chosen as it provides reasonable excitation energies in a set of compounds including charged species and charge-transfer reactions.²²

Because of the complexity of the molecules investigated in the present work, due to the extensive state mixing that occurs in metal complexes, we have also performed CIS calculations²³ in order to check for the reliability of the TD-DFT results. In this case, the computed excitation energies have been scaled by a factor of 0.72 as recommended in the literature.^{24–27} In all cases we have employed the CEP-121G basis set with an extra *f* function on Au.^{28–31}

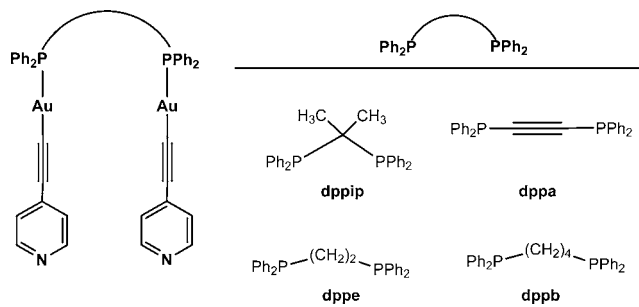
Finally, to check the effect of different environments on the excitation energies, we have performed calculations in gas phase and in solution through the self-consistent reaction field (SCRF) approach.³² In this work, two different solvents have been considered, namely, dichloromethane with dielectric constant ϵ of 8.93 and acetonitrile with dielectric constant ϵ of 35.688.

RESULTS AND DISCUSSION

The series of dinuclear gold(I) (4-pyridyl)ethynyl complexes shown in Scheme 1, differ only in the spacer linking two (identical) arms. The size and geometric features of the spacer is expected to affect the interaction between the two arms and thus affect the photophysical properties that depend on the gold \cdots gold distances.

Absorption. The absorption spectra of the compounds obtained in dichloromethane solution are comparable, as expected by the fact that the chromophoric units ((4-pyridyl)ethynyl and diphenylphosphine) are constant within the series. All the compounds show a vibronically resolved band

Scheme 1



around 280 nm, while in the case of dppip, significant broadening of the bands was observed (Figure 1). The

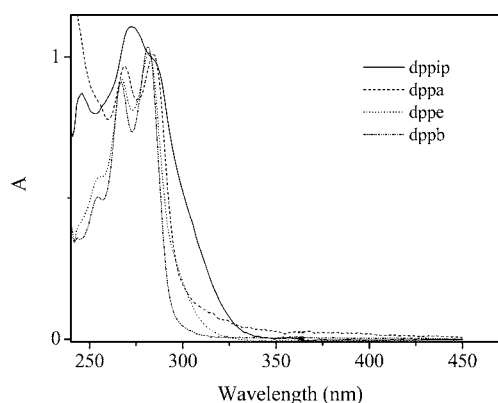


Figure 1. Absorption spectra of the gold(I) (4-pyridyl)ethynyl derivatives studied in this work (in dichloromethane at room temperature). The presence of aurophilic interactions in dppip leads to band broadening due to $\pi-\pi$ stacking of the ethynylpyridine moieties and the appearance of a new band at ~ 310 nm corresponding to a $\sigma^*_{Au-Au} \rightarrow \pi^*$ transition.

broadening was assigned as indicative of $\pi-\pi$ stacking between the (4-pyridyl)ethynyl arms in solution, favored by the existence of aurophilic interactions, which were confirmed by NMR.¹⁷ The presence of a new CT band at ~ 310 nm (corresponding to a $\sigma^*_{Au-Au} \rightarrow \pi^*$ transition, see below) also contributes to the observed band broadening.

In an attempt to rationalize the experimental findings we have carried out a series of calculations on the model system shown in Figure 2. This is a dinuclear gold(I) (4-pyridyl)ethynyl complex in which we have substituted the spacer between the two arms by two methyl groups, one placed in

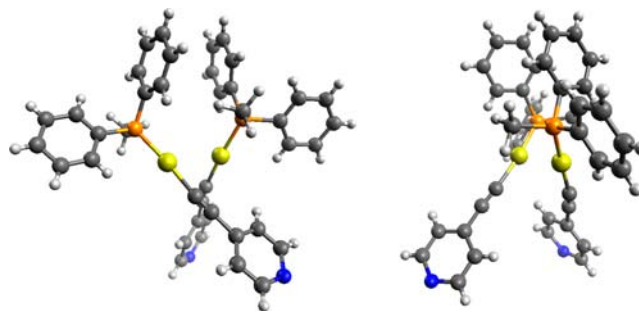


Figure 2. Different projections of the model system employed in the theoretical calculations.

Table 1. Computed Absorption Bands for the Dinuclear Gold(I) (4-Pyridyl)Ethyne Complex Carried out at the Au–Au Distance of 3.0 Å and Experimental Wavelengths at Maximum Absorptions, λ_{max} , in Dichloromethane and Acetonitrile

transition	method	calculated						experimental	
		gas		MeCN		CH ₂ Cl ₂		MeCN	CH ₂ Cl ₂
		exct. ^a	f_{ij} ^b	exct. ^a	f_{ij} ^b	exct. ^a	f_{ij} ^b	$\lambda^{a,d}$	$\lambda^{a,d}$
$\pi \rightarrow \pi$	CAM-B3LYP	243	0.4	238	0.6	239	0.4	279	281
	CIS ^c	298	0.4	300	0.6	302	0.2		
CT	CAM-B3LYP	271	0.2	266	0.3	267	0.4	~300	
	CIS ^c	310	0.5	313	0.8	316	0.9		

^aExcitation and λ_{max} in nm. ^b f_{ij} stands for the computed transition oscillators strength. ^cScaled by 0.72, see text. ^dExperimental values of absorption at maximum obtained for (PPh₃)₂[Au(C≡Cpy)] in dichloromethane and acetonitrile (Figure S1)

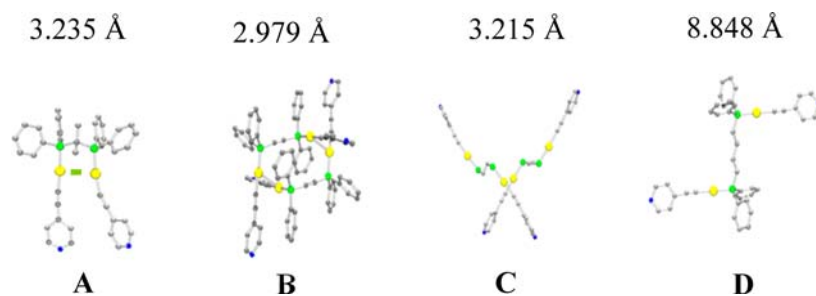


Figure 3. X-ray structures evidencing the shortest gold–gold distances of (A) dppip, (B) dppa, (C) dppe, and (D) dppb derivatives.

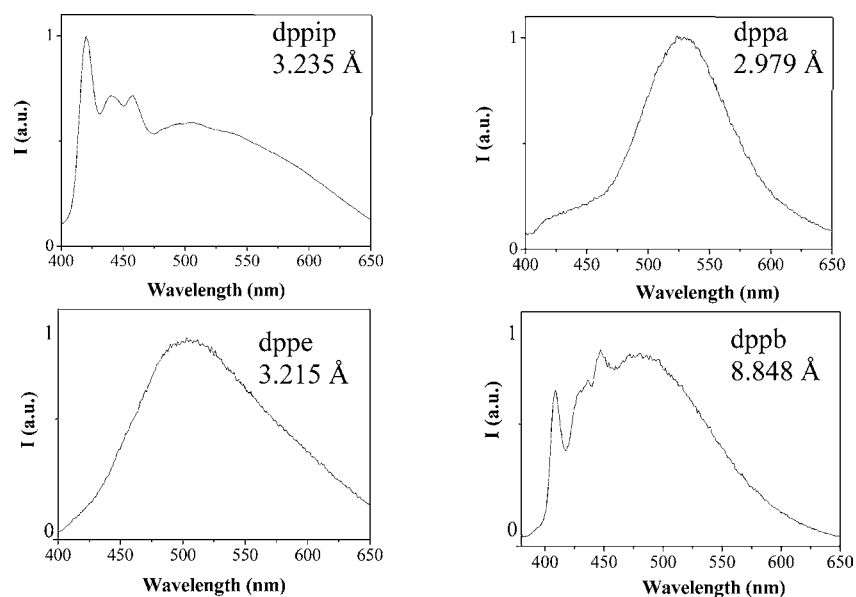


Figure 4. Normalized emission spectra of the solids (a) dppip, (b) dppa, (c) dppe, and (d) dppb derivatives (room temperature; $\lambda_{\text{exc}} = 360$ nm).

each arm. The interaction between the two arms has been modeled simply by modifying the Au–Au distance ($d_{\text{Au–Au}}$). Thus, we have started with the crystal geometry of the dppe gold derivative and we have performed calculations at $d_{\text{Au–Au}} = 3.0, 3.2, 3.4, 3.6,$ and 3.8 Å, without relaxing the geometries.

The model used is obviously a simplification, since the distance is not the only parameter that can impact in the calculated transitions. Among other factors the nature of the bond connecting the arms and the angle between the arms, can also affect the calculated transitions. We decided to use a model where the bond between the arms is absent to have a more general model that could include all situations (in some cases the aurophilic interaction is intramolecular, in others intermolecular, and in one case absent); the simplified model

allows a continuous change of the Au...Au distance. We have studied both the impact of the distance for a given angle and the impact of the angle for the shorter distance (see Table S1 in Supporting Information for the angle dependence) and we have observed that the angle did not had a significant impact in the energy of the calculated transitions.

We have computed the absorption bands for the dinuclear gold(I) (4-pyridyl)ethynyl complex in gas phase and in solution, with acetonitrile and dichloromethane as solvents and using two different methods: CIS and CAM-B3LYP approaches. The corresponding results have been collected in Table 1, which shows that the CIS approach predict a $\pi \rightarrow \pi^*$ band close to 300 nm, in very good agreement with the experimental observation. It mainly corresponds to a transition

between the π bonding and antibonding orbitals of the (4-pyridyl)ethynyl units. In addition, our calculations predict an intense charge transfer (CT) band close to 310 nm, corresponding to a transition from the double occupied HOMO $\sigma_{\text{Au-Au}}^*$ (with antibonding character) to the π^* orbital of pyridine. Table 1 also shows that the CAM-B3LYP approach predict less accurate results in terms of energy, with the $\pi \rightarrow \pi^*$ transition close to 240 nm and the CT transition near 267 nm. However, both theoretical approaches predict qualitatively the same results. The calculations predict that the absorption bands do not depend very much on the solvent which is in agreement with the small shifts observed experimentally for the $\pi \rightarrow \pi^*$ transition (see Table 1 and Supporting Information Figure S1) in the monomeric compound $(\text{PPh}_3)[\text{Au}(\text{C}\equiv\text{Cpy})]$. The CT band, in the case of $(\text{PPh}_3)[\text{Au}(\text{C}\equiv\text{Cpy})]$, can only be clearly seen in acetonitrile, a clear indication that this solvent induces aurophilic interactions (Supporting Information Figure S1), which are absent in dichloromethane solution.

Emission. The emission of the compounds was measured in the solid state, for which the crystallographic data was previously obtained,¹⁷ to correlate the photophysical parameters with the crystallographic gold–gold distance.

For all the compounds, we selected the shortest distance between two gold atoms from X-ray data (Figure 3).

In the case of compound A this distance corresponds to an aurophilic interaction from an intramolecular distance while in compounds B and C corresponds to an intermolecular interaction in a dimeric structure or in a chain respectively. In the case of the dppb derivative (D), the shortest Au–Au distance is longer than the considered for this kind of interactions, that is, structure D does not present aurophilic contacts between gold atoms.

In general, the solids present broad emission bands with distinct features between 425 and 570 nm (Figure 4): a band displaying a well-defined vibrational progression is observed at higher energies in some cases (in the range 425–458 nm) and a second emission band (in the range 500–570 nm) presents a broad structureless shape. Both bands present very large Stokes shifts with respect to the absorption ($>7000 \text{ cm}^{-1}$). Since we are working in solid state, we can discard nuclear relaxation of the excited state as the origin of such a large Stokes shift. This implies that the emission arises from an electronic state that is different from the initial excited state, formed upon absorption. The decaytimes in the order of microseconds (see below) also indicate a forbidden transition to the ground state (states of different spin multiplicity), which is indicative of triplet origin for the observed emissions.

The CAM-B3LYP approach was applied to analyze the dependence of the absorption bands on the Au–Au distance, and our results are collected in Table 2. The calculations predict that the $\pi \rightarrow \pi^*$ transition does not change on increasing the distance between both gold atoms. This result is expected because this transition occurs between orbitals of the ethynylpyridine moiety in each arm, and this is not modified significantly on varying the Au–Au distance. On the other side, our calculations predict that the CT transition changes from 266 nm at $d(\text{Au–Au})$ of 3.0 Å to 238 nm at $d(\text{Au–Au})$ of 3.8 Å. Previously, we have pointed out that this band corresponds to a $\sigma_{\text{Au–Au}}^* \rightarrow \pi^*$ transition, and thus, the $\sigma_{\text{Au–Au}}^*$ orbital energy decreases on increasing the Au–Au distance, because of its antibonding nature. Consequently, the energy gap becomes larger and transition wavelength diminishes.

Table 2. Computed absorption bands for the dinuclear gold(I) (4-pyridyl)ethynyl complex carried out at different Au–Au distances (in Å), using the CAM-B3LYP approach

$d(\text{Au–Au})$	$\pi \rightarrow \pi$		CT	
	exct. ^a	f_{ij}^b	exct. ^a	f_{ij}^b
3.0	238	0.6	266	0.3
3.1	236	0.6	260	0.3
3.2	237	0.5	254	0.3
3.4	236	0.4	246	0.4
3.6	235	0.4	240	0.5
3.8	238	0.6	238	0.6

^aExcitation in nm. ^b f_{ij} stands for the computed transition oscillator strength.

It can be observed from figure 4 that the emission maximum of the broad and structureless band displays a shift to lower energies on increasing the Au–Au distance, despite the fact that the broadness of the band and the different contributions of the structured emission introduce some uncertainty on the position of the maximum. This could indicate that the $^3(\sigma_{\text{Au–Au}}^* \leftarrow \pi^*)$ state does have some contribution to the observed triplet states, probably through state mixing. However, we should remember that dppb, which does not display aurophilic contacts, shows the same type of emission, that is, the observed emission does not arise from the $^3(\sigma_{\text{Au–Au}}^* \leftarrow \pi^*)$ state.

The CIS approach was used to investigate the relative energetic position of up to ten singlet and triplet excited states at $d(\text{Au}\cdots\text{Au})$ of 3.0 and 3.2 Å in gas phase and considering dichloromethane as solvent (the corresponding results are compiled in Supporting Information Table S2). Our calculations predict that all the first ten singlet excited states lie very close in energy (between 290 and 310 nm) confirming the extensive state mixing pointed out above. Please note that, as discussed above and pointed out in Table 1, the observed absorption bands correspond to excitation from the ground singlet state to the first excited singlet state (charge transfer transition at 310 nm with an oscillator strength of 0.5) and to the fourth excited singlet state ($\pi \rightarrow \pi^*$ transition 298 nm with an oscillator strength of 0.4).

Regarding the triplet states, our results predict two different energetic zones, each one with an extensive state mixing too. The first zone lie between 548 and 514 nm and involve the six lowest lying triplet states, whereas the second zone lie between 375 and 368 nm involving four additional triplet states. The extensive state mixing of the excited triplet states investigated is also confirmed by looking at their corresponding electronic features. Although it is not easy to provide a clear electronic characterization, the analysis of the electronic excitations indicates that triplets T1, T2, and T3 involve excitations from the ethynylpyridine orbitals whereas the remaining triplet states involve excitations from the phosphine orbitals. Some of the orbitals involved in the transitions display nonzero coefficients of gold orbitals, but it was not found any contribution of the $\sigma_{\text{Au–Au}}^* \leftarrow \pi^*$ transition in the ten lower triplet states.

The approaching of the gold atoms has noticeable impact in the experimental photophysical parameters obtained for the emission of the triplet states, that is, the measured emission quantum yields and decaytimes change appreciably (see Table 3).

The emission decays collected at different wavelengths are well fitted with a single exponential law and the emission decaytimes measured at several emission wavelengths along the

Table 3. Measured Gold–Gold Distances, Experimental Emission Quantum Yields, Φ_{em} , and Emission Decay Times, τ

compound spacer	Au–Au distance (Å)	Φ_{em}	τ (μ s)
dppa	2.979	0.0120	0.7
dppe	3.215	0.0062	1.2
dppip	3.235	0.0080	1.5
dppb	8.848	0.00005	3.5

broad emission bands show only differences assignable to the experimental uncertainty. This implies that the broad emissions arise from thermally equilibrated triplet states.

The most interesting finding is the clear correlation between the decaytimes and the Au...Au distances up to ~ 8 Å; the shorter the distance the shorter the decaytime. This decrease in the decaytime with the decrease in gold–gold distance is accompanied by an opposite correlation of the emission quantum yield, which increases with decreasing distance (see Table 4).

Table 4. Average Radiative, k_r , and Non-radiative, k_{nr} , Rate Constants of the Triplet Emissive States

compound spacer	k_r (10^3 s $^{-1}$)	k_{nr} (10^5 s $^{-1}$)
dppa	17.14	14.11
dppe	5.17	8.28
dppip	5.30	6.61
dppb	0.01	2.86

The interpretation is straightforward: the chromophores display an efficient channel for the deactivation of the lowest triplet states whose efficiency increases with the shortening of the Au...Au distance, as displayed by the decrease in decaytimes.

The radiative and nonradiative rate constants were calculated from the decaytimes and emission quantum yields, using eqs 1–4

$$\Phi_{em} = \eta_{isc} \times \frac{k_r}{k_r + k_{nr}} \quad (1)$$

$$\tau = \frac{1}{k_r + k_{nr}} \quad (2)$$

$$k_r = \frac{\Phi_{em}}{\tau} \quad (3)$$

$$k_{nr} = \frac{1}{\tau} - k_r \quad (4)$$

where η_{isc} accounts for the efficiency of triplet formation from the excited singlet state, which we can assume to be close to one, since all emission observed is assigned to triplet states. The results are summarized in Table 4 and show that both rate constants (radiative and nonradiative) increase on decreasing the Au–Au distance.

While the nonradiative rate increases 5 times, the radiative rate increases ~ 1700 times on decreasing the gold–gold distance from 8 to 2.978 Å. The net effect is a radiative increase. The approaching of both gold atoms leads to the increase on intersystem crossing to the ground state, a consequence of spin–orbit coupling induced by the approaching of an additional “heavy atom” (gold atom from the second arm).

The overall effect of the Au...Au approximation is an increase in phosphorescence emission. This has led to the generalized idea that the aurophilic interactions give rise to the observed low energy emissions; aurophilic interactions intensify the emissions.

The absence of a $\sigma_{Au-Au}^* \leftarrow \pi^*$ transition in the calculated emissive states has been generating some controversy in the interpretation of the luminescence of gold compounds.^{33–38} This radiative increase provides a general explanation on why stronger emission of gold compounds is observed in the cases where aurophilic interactions are present, even in the cases where theoretical calculations do not show $\sigma_{Au-Au}^* \leftarrow \pi^*$ transitions as the lowest emissive states.

From a strictly phenomenological point of view, the increase in k_r implies that the spin-forbidden transition becomes more allowed, which in turn implies the involvement of a spin–orbit coupling mechanism. On the other hand, the spin–orbit coupling requires that the electrons “see” the approaching gold atom, or in other words, in the emissive excited state one of the half-filled molecular orbitals must have a nonzero coefficient of the atomic orbitals of the approaching gold atoms. This is like saying that one of the electrons must be in a molecular orbital which includes some electronic density in both gold atoms. It is clear that spin–orbit coupling will be much more efficient when all the density is located in both gold atoms, such as in the σ_{Au-Au}^* molecular orbital involved in the $\sigma_{Au-Au}^* \leftarrow \pi^*$ transition, but it is not strictly necessary to be so.

Despite that this conclusion applies strictly to the set of compounds in this manuscript, we think that some generalizations are allowed.

In some of the compounds studied the aurophilic interaction is intramolecular, in others intermolecular, and in the last case absent. The fact that the photophysical parameters do not seem to depend on “through bond” effects and correlated well with the Au...Au distance seems to point in favor of a distance dependent heavy atom effect, or to the participation of Au...Au centered orbitals in the observed transitions, affecting the photophysical parameters (k_r and k_{nr}). However, note that the “quality” of the emissive state is the same in the case where the gold atoms are very separated (dppb, where aurophilic contacts are absent), only the “quantity” of light emitted is lower, that is, the emissive state is not an Au...Au centered transition.

In summary, the approaching of the gold centers will increase the spin–orbit-coupling (and the radiative rate constant of the lowest triplet state). In all cases where the radiative rate constant is higher than the nonradiative rate constant (e.g., solid state and low temperatures) an increase in phosphorescence emission accompanies the decrease in Au...Au distance. This rationale does not need to specify the nature of the lowest emissive states, which are difficult to determine due to extensive state mixing, and relies on general photophysical laws, i.e., it is not necessary to invoke unique spectroscopic features in the absorption and emission related to the presence of $\sigma_{Au-Au}^* \leftarrow \pi^*$ transitions.

CONCLUSIONS

The analysis of the theoretical calculations and emission features of a series of alkylnyl gold(I) complexes with the same chromophoric unit ((4-pyridyl)ethynyl) let us to demonstrate that there is not a straightforward correlation between the presence of a $\sigma_{Au-Au}^* \leftarrow \pi^*$ transition and the presence or absence of an emission band.

However, the calculation of the emission quantum yields together with the emission decay times show that the shorter the gold–gold distance the higher the radiative rate constant and emission quantum yield, due to the increase on intersystem crossing to the ground state, promoted by the approaching of the two gold atoms.

The approach of the gold centers will increase the spin–orbit-coupling and the calculated radiative constants are clearly higher for shorter Au···Au distances, which is in agreement with the generalized idea that the aurophilic interaction favors luminescence in gold compounds. This is not related with the exact nature of the lowest triplet states but with a more general photophysical effect which turns the radiative transitions more allowed, with consequent increase of the phosphorescence emission.

■ ASSOCIATED CONTENT

■ Supporting Information

Cartesian coordinates of dppe derivative; absorption spectra of $(\text{PPh}_3)_2[\text{Au}(\text{C}\equiv\text{Cpy})]$ compound in dichloromethane and acetonitrile (Figure S1); computed relative energy position (in CH_2Cl_2) of the first ten excited singlet and triplet electronic states for the dinuclear gold(I) ethynylpyridine model carried out at $d(\text{Au}–\text{Au}) = 3.2 \text{ \AA}$, and changing the angle between the arms (CIS approach) (Table S1); computed relative energy position of the first ten excited singlet and triplet electronic states for the dinuclear gold(I) ethynylpyridine model carried out at $d(\text{Au}–\text{Au}) = 3.0 \text{ \AA}$, using the CIS approach (Table S2). This material is available free of charge via the Internet at <http://pubs.acs.org>.

■ AUTHOR INFORMATION

Corresponding Author

*Fax: +351 212948550. Tel: +351 212948300 (Ext. 10923). E-mail: lima@fct.unl.pt

Notes

The authors declare no competing financial interest.

■ ACKNOWLEDGMENTS

The support and sponsorship provided by COST Action CM1005 is acknowledged. Authors are also grateful to the Ministerio de Ciencia e Innovación of Spain (Project CTQ2009-08795), the Generalitat de Catalunya (Grant 2009SGR01472) and Fundação para a Ciência e Tecnologia of Portugal (PTDC/QUI-QUI/112597/2009). The computer services of the CESCA are also acknowledged.

■ REFERENCES

- (1) Comprehensive Supramolecular Chemistry ; Atwood, J. L., Davies, J. E. D., MacNicol, D. D., Vögtle, F., Suslick, K. S., Eds.; Pergamon Press: Oxford, U.K., 1996.
- (2) Pitzer, K. S. *Acc. Chem. Res.* **1979**, *12*, 272.
- (3) Yam, V. W.-W.; Cheng, E. C.-C. *Chem. Soc. Rev.* **2008**, *37*, 1806.
- (4) Schmidbaur, H.; Schier, A. *Chem. Soc. Rev.* **2012**, *41*, 370.
- (5) Pyykkö, P. *Chem. Rev.* **1997**, *97*, 597.
- (6) Pyykkö, P. *Angew. Chem., Int. Ed.* **2004**, *43*, 4412.
- (7) Pyykkö, P. *Inorg. Chim. Acta* **2005**, *358*, 4113.
- (8) Fernández, E. J.; López-de-Luzuriaga, J. M.; Monge, M.; Rodríguez, M. A.; Crespo, O.; Gimeno, M. C.; Laguna, A.; Jones, P. G. *Chem.—Eur. J.* **2000**, *6*, 636.
- (9) Laguna, A.; Lasanta, T.; López-de-Luzuriaga, J. M.; Monge, M.; Naumov, P.; Olmos, M. E. *J. Am. Chem. Soc.* **2010**, *132*, 456.

- (10) Fernández, E. J.; Hardacre, C.; Laguna, A.; Lagunas, M. C.; López-de-Luzuriaga, J. M.; Monge, M.; Montiel, M.; Olmos, M. E.; Puellas, R. C.; Sánchez-Forcada, E. *Chem.—Eur. J.* **2009**, *15*, 6222.
- (11) Yam, V. W.-W.; Lo, K. K.-W. *Chem. Soc. Rev.* **1999**, *28*, 323.
- (12) Fernández, E. J.; Laguna, A.; López-de-Luzuriaga, J. M. *Dalton Trans.* **2007**, 1969.
- (13) Yam, V. W.-W.; Lo, K. K.-W.; Wong, K. M.-C. *J. Organomet. Chem.* **1999**, *578*, 3.
- (14) Chan, C.-W.; Cheng, L.-K.; Che, C.-M. *Coord. Chem. Rev.* **1994**, *132*, 87.
- (15) Yam, V. W.-W. *Acc. Chem. Res.* **2002**, *35*, 555.
- (16) Wong, K.M.-C.; Yam, V.W.-W. *Coord. Chem. Rev.* **2007**, *251*, 2477.
- (17) Ferrer, M.; Gutiérrez, A.; Rodríguez, L.; Rossell, O.; Lima, J. C.; Font-Bardía, M.; Solans, X. *Eur. J. Inorg. Chem.* **2008**, 2899.
- (18) Lima, J. C.; Rodríguez, L. *Chem. Soc. Rev.* **2011**, *40*, 5442.
- (19) Rodríguez, L.; Lima, J. C. *Global J. Inorg. Chem.* **2011**, *2*, 39–76.
- (20) Frisch, M. J.; Trucks, G. W.; Schlegel, H. B.; Scuseria, G. E.; Robb, M. A.; Cheeseman, J. R.; Scalmani, G.; Barone, V.; Mennucci, B.; Petersson, G. A.; Nakatsuji, H.; Caricato, M.; Li, X.; Hratchian, H. P.; Izmaylov, A. F.; Bloino, J.; Zheng, G.; Sonnenberg, J. L.; Hada, M.; Ehara, M.; Toyota, K.; Fukuda, R.; Hasegawa, J.; Ishida, M.; Nakajima, T.; Honda, Y.; Kitao, O.; Nakai, H.; Vreven, T.; Montgomery, J. A., Jr.; Peralta, J. E.; Ogliaro, F.; Bearpark, M.; Heyd, J. J.; Brothers, E.; Kudin, K. N.; Staroverov, V. N.; Kobayashi, R.; Normand, J.; Raghavachari, K.; Rendell, A.; Burant, J. C.; Iyengar, S. S.; Tomasi, J.; Cossi, M.; Rega, N.; Millam, J. M.; Klene, M.; Knox, J. E.; Cross, J. B.; Bakken, V.; Adamo, C.; Jaramillo, J.; Gomperts, R.; Stratmann, R. E.; Yazyev, O.; Austin, A. J.; Cammi, R.; Pomelli, C.; Ochterski, J. W.; Martin, R. L.; Morokuma, K.; Zakrzewski, V. G.; Voth, G. A.; Salvador, P.; Dannenberg, J. J.; Dapprich, S.; Daniels, A. D.; Farkas, Ö.; Foresman, J. B.; Ortiz, J. V.; Cioslowski, J.; Fox, D. J. *Gaussian*; Gaussian, Inc.: Wallingford CT, 2009.
- (21) Yanai, T.; Tew, D. P.; Handy, N. C. *Chem. Phys. Lett.* **2004**, *393*, 519.
- (22) Goerigk, L.; Grimme, S. *J. Chem. Phys.* **2010**, *132*, 184103.
- (23) Foresman, J. B.; Head-Gordon, M.; Pople, J. A.; Frisch, M. J. *J. Phys. Chem.* **1992**, *96*, 135.
- (24) Broo, A.; Holmén, A. *J. Phys. Chem. A* **1997**, *101*, 3589.
- (25) Shukla, M. K.; Leszczynski, J. *J. Phys. Chem. A* **2002**, *106*, 1011.
- (26) Broo, A. *J. Phys. Chem. A* **1998**, *102*, 526.
- (27) Li, J.; Pyykkö, P. *Chem. Phys. Lett.* **1992**, *197*, 586.
- (28) Holmén, A.; Broo, A.; Albinsson, B.; Nordén, B. *J. Am. Chem. Soc.* **1997**, *119*, 12240.
- (29) Stevens, W. J.; Basch, H.; Krauss, M. *J. Chem. Phys.* **1984**, *81*, 6026.
- (30) Stevens, W. J.; Krauss, M.; Basch, H.; Jasien, P. G. *Can. J. Chem.* **1992**, *70*, 612.
- (31) Cundari, T. R.; Stevens, W. J. *J. Chem. Phys.* **1993**, *98*, 5555.
- (32) Tomasi, J.; Mennucci, B.; Cammi, R. *Chem. Rev.* **2005**, *105*, 2999.
- (33) Lim, S. H.; Olmstead, M. M.; Balch, A. L. *J. Am. Chem. Soc.* **2011**, *133*, 10229.
- (34) Ovens, J. S.; Truong, K. N.; Leznoff, D. B. *Dalton Trans.* **2012**, *41*, 1345.
- (35) van Zyl, W. E.; López-de-Luzuriaga, J. M.; Mohamed, A. A.; Staples, R. J.; Fackler, J. P., Jr. *Inorg. Chem.* **2002**, *41*, 4579.
- (36) Assefa, Z.; Omary, M. A.; McBurnett, B. G.; Mohamed, A. A.; Patterson, H. H.; Staples, R. J.; Fackler, J. P., Jr. *Inorg. Chem.* **2002**, *41*, 6274.
- (37) Hunks, W. J.; Lapierre, J.; Jenkins, H. A.; Puddephatt, R. J. *J. Chem. Soc., Dalton Trans.* **2002**, 2885.
- (38) Wing-Wah Yam, V.; Kam-Wing Lo, K. *Chem. Soc. Rev.* **1999**, *28*, 323.